High mechanical and thermoelectric performances in hot-pressed CdO

M. A. Madre*, M. A. Torres, A. Sotelo

ICMA (Universidad de Zaragoza-CSIC), Dpto. de Ciencia y Tecnología de Materiales y Fluidos, C/María de Luna 3, E-50018-Zaragoza, Spain

Abstract

High density bulk CdO polycrystalline thermoelectric ceramics have been prepared through a hot-pressing process. Density measurements have revealed that density reaches 99.5 % of the theoretical one, in agreement with the observed microstructure. Microhardness has shown to have indentation size effect, decreasing when the load is raised. Electrical resistivity shows metallic-like behaviour until 650 ºC and semiconducting-like at higher temperatures while Seebeck coefficient increases in the metallic-like region and decreases in the semiconducting one. The maximum power factor values, 1.6 mW/K^2m, have been achieved at about 650 ºC. These values are the highest obtained in this family of materials, with the advantage of its low thermal treatment duration, when compared with the typical solid state sintering process.

Keywords: Hot-pressing; Hardness test; Electrical resistivity; Power factor; CdO

Corresponding author: M. A. Madre

e-mail: amadre@unizar.es

Address: C/Maria de Luna, 3. 50018-Zaragoza (Spain)

Tel: +34 976762617

Fax: +34 976761957

1. Introduction

The energetic crisis periodically shaking the world economy clearly pushes up the research for more efficient or new energy sources. In this context, thermoelectric (TE) materials can play an important role in renewable energy generation [1] or harvesting the wasted heat in other energy transforming systems [2]. In this last case, they can increase the efficiency, decreasing the fossil fuels consumption helping to fight, at the same time, against global warming. On the other hand, for all these applications it is necessary to produce high performance materials, quantified through the dimensionless Figure-of-Merit, ZT ($=TS^2/\rho\kappa$, where S is Seebeck coefficient, ρ electrical resistivity, κ thermal conductivity, and T absolute temperature [3]).

Nowadays, the practical applications of TE devices are limited to materials which display high ZT values at relatively low temperatures [4-6]. As a consequence, the niche applications of these materials are strongly limited by temperature. Nevertheless, in 1997 these temperature limitations were surpassed by the discovery of attractive TE properties in $Na_2Co_2O_4$ ceramics [7]. From this moment on, many works have been published on CoO-based materials [8-14] with hole conduction behavior. On the other hand, the search for a high performance TE material with electronic conduction behavior is being performed in different systems, as TiO-, or MnO-based ones [15,16], while very few works are being conducted in other materials, such as CdO [17-19].

CdO can be described using a rock-salt structure with $Fm\bar{3}m$ space group [20] and possess a sublimation point of 1559 ºC [21]. This last parameter can drastically influence the processing conditions, even if relatively high density materials can be produced when sintered at relatively low temperatures [22]. As

a consequence, some processes producing very high density and highly conductive ceramics via melt-solidification [23,24] are unuseful due to the absence of a liquid phase. However, some methods have been reported to produce high density materials at relatively low temperatures when applied to other ceramic systems, as hot uniaxial pressing [25], or spark plasma sintering [26]. This improvement in density produces better grains connectivity, which is reflected in a drastic decrease of the materials electrical resistivities.

Taking into account the material's characteristics previously presented, the aim of this work is producing high density CdO material. The effect of hot-pressing process on its mechanical, microstructural, and thermoelectric characteristics will be studied and compared with the reported values in the literature.

2. Experimental

CdO (99%, Panreac) commercial powder was used as starting material without any previous preparation. It was uniaxially pressed at around 400 MPa to produce green ceramic disks of 25 mm diameter and 3 mm thick. These compacts were then hot-pressed under air at 800 ºC and around 30 MPa applied pressure during 6 h with a final furnace cooling. The resulting disks (about 26 mm diameter and 2.5 mm thick) were then cut into pieces with the adequate dimensions for their subsequent characterization.

Microstructural observations were performed on transversal fractured surfaces using a Field Emission Scanning Electron Microscope (FESEM, Carl Zeiss Merlin). Apparent density determinations have been made on several samples, measuring each one for three times to minimize measurement errors. These data were compared with the theoretical density of this compound, 8.15 g/cm^3

[21]. Mechanical characterization has been made using a Vickers indentation system (Matsuzawa MXT70). Microhardness of several samples has been determined using different applied loads, ranging between 0.245 and 9.81 N, with 15 seconds dwell time.

Electrical resistivity and Seebeck coefficient were simultaneously determined by the standard dc four-probe technique in a LSR-3 measurement system (Linseis GmbH), in the steady state mode and at temperatures ranging from 50 to 800 ºC under He atmosphere. With the electrical resistivity and Seebeck coefficient data, the power factor has been calculated in order to determine the samples performances.

3. Results and discusion

SEM micrographs performed on representative transversal fractures sections of samples are presented in Fig. 1. In the micrographs, it can be clearly seen that samples are composed by very regular grains, without apparent porosity when observed at high magnification (Fig. 1a). When the fractures are observed at higher magnification (Fig. 1b), some porosity can be observed in the surface of grains. Moreover, in spite of some residual porosity observed in the grain boundaries, they seem to be very clean surfaces between adjacent grains.

In order to confirm the low porosity observed in SEM micrographs, apparent density measurements have been performed in the hot-pressed samples. The obtained values are around 99.5 % of CdO theoretical density, with 0.14 g/cm^3 standard error, clearly confirming the very low porosity content in these samples. These values are higher than the reported in the literature for solid

state sintered samples at 800 and 900 ºC (97.7, and 98.7 %, respectively) [19,27,28].

Vickers hardness of samples has been determined using the following equation:

$$HV = 1.8544 \times \frac{(F \times 9.81)}{d^2} \qquad \text{(eq, 1)}$$

HV is the microhardness in MPa, (*F x* 9.81*)* is the applied load in N, and *d* is the vertical and horizontal diagonals mean value of each indentation, in mm. The obtained results, together with their standard error, as a function of the applied load, is presented in Fig. 2. As it can be clearly observed in the graph, the hardness is clearly depending on the applied load, decreasing with logarithmic trend with the load. This behaviour is the typical determined in similar ceramic systems [29,30]. The data were analysed according to Meyer's law [31]:

$F = A\, d^n$ (eq. 2)

where *F* is the applied load, *d* the indentation diagonal length, *n* Meyer's number, and *A* is the standard hardness constant. As it is well known, the *n* value allows distinguishing between the indentation size effect (ISE) and the reverse indentation size effect (RISE). ISE behaviour is found when $n < 2$ and hardness decreases when the applied load is raised. On the other hand, the RISE occurs when $n > 2$, and hardness increases with the applied load. In order to confirm the harness behaviour in these samples, Meyer's number has been determined using the slope of the *ln F-ln d* curve, leading to a value around 0.5, clearly indicating an ISE behaviour in these samples, in agreement with the hardness evolution with the applied load.

The temperature dependence of electrical resistivity is shown in Fig. 3. The ρ (T) curves show a metallic-like behaviour ($d\rho/dT < 0$) from room temperature to about 700 ºC and a semiconducting-like one ($d\rho/dT > 0$) at higher temperatures,

in agreement with the observed behaviour in solid state sintered materials [17,19,32]. This behaviour has been associated to an extrinsic regime at low temperatures (< 700 ºC) where the charge carrier density has been found to be nearly independent of temperature. In this temperature range, the samples exhibit a strong temperature dependence which can suggest that phonon scattering is the main carrier scattering mechanism [33] explaining the raise in electrical resistivity. On the other hand, the decrease found at higher temperatures (> 700 ºC) is due to the promotion of thermally excited intrinsic carriers through the energy gap [34]. In any case, the measured value at room temperature in the hot-pressed materials (1.3 mΩ.cm) is much lower than the best reported in the literature for the solid state sintered pure CdO (11 mΩ.cm) [19] and still lower than the lowest measured in Er- or Pr-doped CdO (2 mΩ.cm) [17,18]. When considering the high temperature values, the measured in the materials prepared in this work (1.3 mΩ.cm at 800 ºC) are much lower than the obtained in sintered materials at similar temperature (18 mΩ.cm) and about the half of the best measured in Er- or Pr-doped materials (4 mΩ.cm) [17,18]. The very low electrical resistivity values obtained in the hot-pressed materials is partially due to the higher density of these materials, compared with the obtained in sintered materials, as previously discussed. The other factor which can decrease electrical resistivity is the applied pressure during the hot-pressing process which can lead to electrically improved grain boundaries.

Fig. 4 displays the variation of the Seebeck coefficient with temperature. In the graph, it can be clearly seen that the sign of the Seebeck coefficient is negative in the whole measured temperature range, which confirms a conduction mechanism mainly governed by electrons. Moreover, the Seebeck coefficient

shows the same behaviour observed in the electrical resistivity, it increases from room temperature until around 700 ºC, and decreases at higher temperatures. This evolution clearly fits with the electrical resistivity discussion, it increases within the extrinsic carriers temperature range and decreases in the intrinsic one. The room temperature values (-75 μV/K) are of the order of the obtained in solid state sintered pure CdO (between -60 and -75 μV/K) [17,19], but lower than the best measured in Ba-doped materials (-160 μV/K) [27]. When considering the values at 800 ºC (-172 μV/K), they are still higher than the measured in solid state sintered undoped materials (between -140 and -160 μV/K) [17,19], and only lower than the measured in Ba-doped CdO (-210 μV/K) [27].

In order to evaluate the thermoelectric performances of these materials, power factor has been calculated from the ρ and S data, and presented in Fig. 4, as a function of temperature. As it can be observed in the plot, PF follows the same trend observed in the electrical resistivity and Seebeck coefficient, it increases from room temperature to about 650 ºC, and decreases at higher temperatures. The values determined at room temperature (0.42 mW/K^2m) are higher than the measured in pure and doped sintered materials (between 0.3 and 0.4 mW/K^2m) [17-19,27,32], with the only exception of the Ni-doped CdO (0.5 mW/K^2m) [22]. Moreover, the maximum PF values measured in this work (1.63 mW/K^2m) are the highest ones obtained in pure and doped CdO ceramics, being about 10 % higher than the best reported values in the literature (1.5 mW/K^2m) [22]. Even if these improvements seem to be not very impressive, it is worth to mention that the samples prepared in this work have been thermally treated for 6 h under

pressure, while the typical thermal treatment in the solid state sintering process is performed for 20 h.

4. Conclusions

In summary, this paper demonstrates that very high density CdO samples can be prepared by a hot-pressing process in a relatively short thermal treatment. Microstructure has shown very small amount of porosity, confirmed through apparent density. The raise in density, together with an improvement in grains connectivity induced by pressure, has led to very low electrical resistivity values, without a drastic decrease of Seebeck coefficient, when compared with literature data. All these factors have led to the highest PF values obtained in this ceramic family, about 10 % higher than the best reported values. Moreover, mechanical properties have shown an ISE behaviour, with relatively high hardness values. Furthermore, these improvements have been produced with a decrease of the thermal treatment duration, usually for 20 h, while in this work 6 h have been used. As a consequence, it can be easily deduced that the processing method used in this work could easily produce high performance TE materials for practical applications.

Acknowledgements

This research has been supported by the Spanish MINECO-FEDER (MAT2013-46505-C3-1-R). The authors wish to thank the Gobierno de Aragón-FEDER (Consolidated Research Groups T12 and T87) for financial support. Authors would like to acknowledge the use of Servicio General de Apoyo a la Investigación-SAI, Universidad de Zaragoza.

References

1. H. Naito, Y. Kohsaka, D. Cooke, H. Arashi, Solar Energy **58**, 191 (1996).

2. G. Mahan, B. Sales, J. Sharp, Phys. Today **50**, 42 (1997).

3. D. M. Rowe, Thermoelectrics Handbook: Macro to Nano, first ed., CRC Press, Boca Raton, 2006.

4. J. M. Santamaria, J. Alkorta, J. G. Sevillano, Bol. Soc. Esp. Ceram. V. **52**, 137 (2013).

5. H. C. Wang, J.-H. Bahk, C. Kang, J. Hwang, K. Kim, J. Kim, P. Burke, J. E. Bowers, A. C. Gossard, A. Shakouri, W. Kim, P. Natl. Acad. Sci. USA **111**, 10949 (2014).

6. H. C. Wang, J. Hwang, M. L. Snedaker, I.-H. Kim, C. Kang, J. Kim, G. D. Stucky, J. Bowers, W. Kim, Chem. Mater. **27**, 944 (2015).

7. I. Terasaki, Y. Sasago, K. Uchinokura, Phys. Rev. B **56**, 12685 (1997).

8. Y. Huang, B. Zhao, J. Fang, R. Ang, Y. Sun, J. Appl. Phys. **110**, 123713 (2011).

9. J. C. Diez, Sh. Rasekh, M. A. Madre, E. Guilmeau, S. Marinel, A. Sotelo, J. Electron. Ceram. **39**, 1601 (2010).

10. J. J. Shen, X. X. Liu, T. J. Zhu, X. B. Zhao, J. Mater. Sci. **44**, 1889 (2009).

11. G. Constantinescu, Sh. Rasekh, M. A. Torres, M. A. Madre, J. C. Diez, A. Sotelo, Scr. Mater. **68**, 75 (2013).

12. K. Rubesova, T. Hlasek, V. Jakes, S. Huber, J. Hejtmanek, D. Sedmidubsky, J. Eur. Ceram. Soc. **35**, 525 (2015).

13. I. V. Matsukevich, A. I. Klyndyuk, E. A. Tugova, A. N. Kovalenko, A. A. Marova, N. S. Krasutskaya, Inog. Mater. **52**, 593 (2016).

14. A. Sotelo, M. A. Torres, G. Constantinescu, Sh. Rasekh, J. C. Diez, M. A. Madre, J. Eur. Ceram. Soc. **32**, 3745 (2012).

15. J. Liu, C. L. Wang, W. B. Su, H. C. Wang, J. L. Zhang, L. M. Mei, Acta Phys. Sinica **60**, 087204 (2011).

16. Y. C. Zhou, C. L. Wang, W. B. Su, J. Liu, H. C. Wang, J. C. Li, Y. Li, J. Z. Zhai, Y. C. Zhang, L. M. Mei, J. Alloys Compds. **680**, 129 (2016).

17. S. Wang, F. Liu, Q. Lu, S. Dai, J. Wang, W. Yu, G. Fu, J. Eur. Ceram. Soc. **33**, 1763 (2013).

18. S. Wang, Q. Lu, L. Li, G. Fu, F. Liu, S. Dai, W. Yu, J. Wang, Scr. Mater. **69**, 533 (2013).

19. X. Zhang, H. Li, J. Wang, J. Adv. Ceram. **4**, 226 (2015).

20. I. Khan, I. Ahmad, B. Amin, G. Murtaza, Z. Ali, Physica B **406**, 2509 (2011).

21. C. R. Hammond, CRC Handbook of chemistry and physics, 90th ed., CRC Press, Boca Raton, 2006.

22. L. Gao, S. Wang, R. Liu, S. Zhai, H. Zhang, J. Wang, G. Fu, J. Alloys Compds. **662**, 213 (2016).

23. F. M. Costa, N. M. Ferreira, Sh. Rasekh, A. J. S. Fernandes, M. A. Torres, M. A. Madre, J. C. Diez, A. Sotelo, Cryst. Growth Des. **15**, 2094 (2015).

24. Sh. Rasekh, G. Constantinescu, M. A. Torres, M. A. Madre, J. C. Diez, A. Sotelo, Adv. Appl. Ceram. **111**, 490 (2012)

25. H. Wang, X. Sun, X. Yan, D. Huo, X. Li, J.-G. Li, X. Ding, J. Alloys Compds. **582**, 294 (2014).

26. J. G. Noudem, R. Retoux, S. Lanfredi, J. Alloys Compds. **676**, 499 (2016).

27. I. Khan, I. Ahmad, B. Amin, G. Murtaza, Z. Ali, Physica B **406**, 2509 (2011).

28. L. Gao, S. Zhai, R. Liu, N. Fu, J. Wang, G. Fu, S. Wang, J. Am. Ceram. Soc. **98**, 3285 (2015).

29. F. Kahraman, J. Mater. Sci.: Mater. Electron. **27**, 8006 (2016).

30. B. Ozkurt, J. Supercond. Nov. Magn. **27**, 2407 (2014).

31. E. Meyer, Z. Ver. Deut. Ing. **52**, 740 (1908).

32. Q. Lu, S. Wang, L. J. Li, J. Wang, S. Dai, W. Yu, G. Fu, Sci. China **57**, 1644 (2014).

33. S. Ohta, T. Nomura, H. Ohta, K. Koumoto, J. Appl. Phys. **97**, 034106 (2005).

34. L. A. Kuznetsova, V. L. Kuznetsov, D. M. Rowe, J. Phys. Chem. Solids **61**, 1269 (2000).

Figure captions:

Figure 1. SEM micrographs performed on representative transversal fractured sections of CdO samples at a) low; and b) high magnification.

Figure 2. Evolution of Vickers hardness, determined in hot-pressed CdO samples, with the applied load. The line is a guide for the eye.

Figure 3. Temperature dependence of electrical resistivity in CdO hot-pressed samples.

Figure 4. Temperature dependence of Seebeck coefficient in CdO hot-pressed samples.

Figure 5. Temperature dependence of power factor in CdO hot-pressed samples.

Figure 1

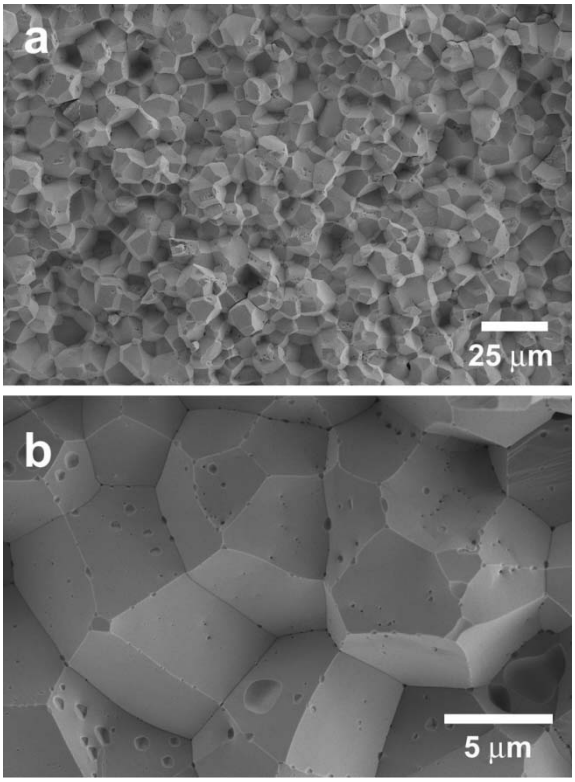

Figure 2

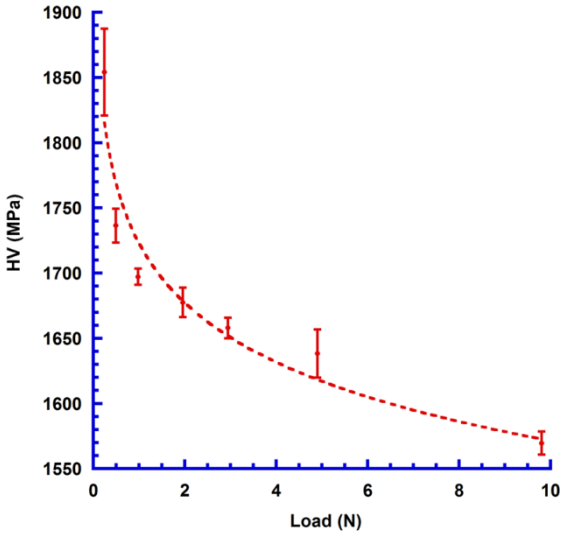

Figure 3

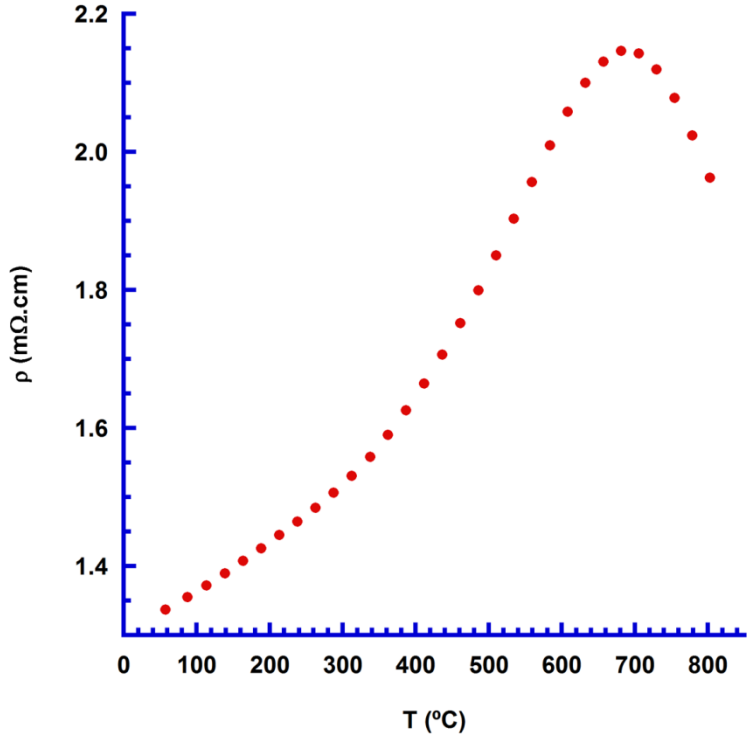

Figure 4

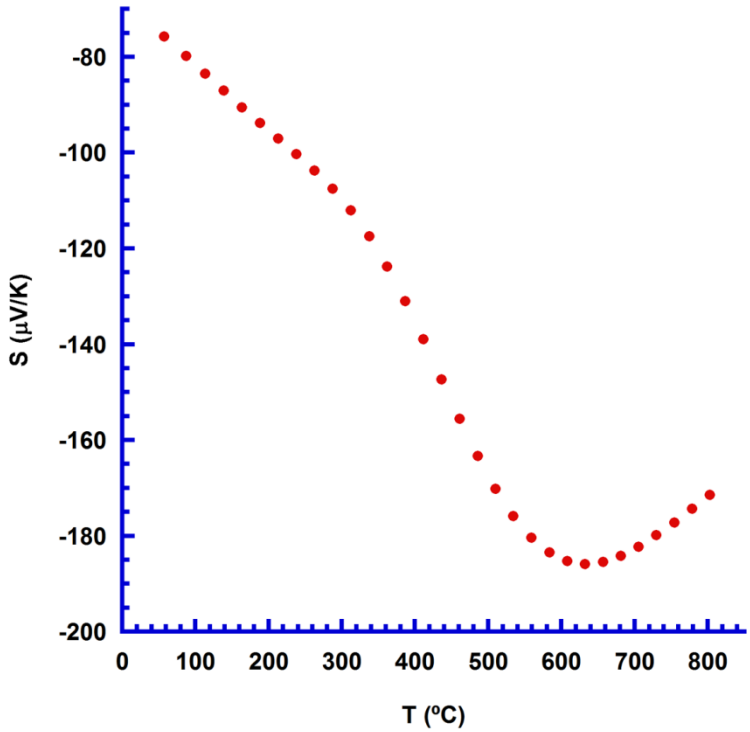
-80
-100
-120
-140
-160
-180
-200
S (μV/K)
0
100
200
300
400
500
600
700
800
T (°C)

Figure 5